

1 **A divergent hepatitis D-like agent in birds**

2

3

4 Michelle Wille^{1,*,#}, Hans J. Netter², Margaret Littlejohn², Lilly Yuen², Mang Shi³, John-
5 Sebastian Eden³, Marcel Klaassen⁴, Edward C. Holmes³, and Aeron C. Hurt¹.

6

7

8 ¹WHO Collaborating Centre for Reference and Research on Influenza, The Peter Doherty
9 Institute for Infection and Immunity, Melbourne, Victoria, Australia

10 ²Molecular Research and Development, Victorian Infectious Diseases Reference Laboratory,
11 Royal Melbourne Hospital at the Peter Doherty Institute for Infection and Immunity,
12 Melbourne, Victoria, Australia

13 ³Marie Bashir Institute for Infectious Diseases and Biosecurity, Charles Perkins Centre,
14 School of Life and Environmental Sciences and Sydney Medical School, The University of
15 Sydney, Sydney, NSW 2006, Australia

16 ⁴Centre for Integrative Ecology, Deakin University, Geelong, Victoria, Australia

17 *Corresponding author: michelle.wille@influenzacentre.org

18

19 **Running Title:** Hepatitis D-like agent in birds

20

21 Abstract Word Count: 100

22 Text Word Count: excluding references, table footnotes and figure legends: 2068

23 Number of Figures: 4

24

25

26

27 **Abstract**

28 Hepatitis delta virus (HDV) is currently only found in humans, and is a satellite virus that
29 depends on hepatitis B virus (HBV) envelope proteins for assembly, release and entry. Using
30 meta-transcriptomics, we identified the genome of a novel HDV-like agent in ducks.
31 Sequence analysis revealed secondary structures that were shared with HDV, including self-
32 complementarity and ribozyme features. The predicted viral protein shares 32% amino acid
33 similarity to the small delta antigen of HDV and comprises a divergent phylogenetic lineage.
34 The discovery of an avian HDV-like agent has important implications for the understanding
35 of the origins of HDV and subviral agents.

36

37 **Importance**

38 Hepatitis delta virus (HDV) is currently only found in humans, and coinfections of HDV and
39 Hepatitis B virus (HBV) in humans result in severe liver disease. There are a number of
40 hypotheses for the origin of HDV, although a key component of all is that HDV only exists in
41 humans. Here, we describe a novel deltavirus-like agent identified in wild birds. Although
42 this agent is genetically divergent, it exhibits important similarities to HDV, such as the
43 presence of ribosymes and self-complementarity. The discovery of an avian HDV-like agent
44 challenges our understanding of both the origin and the co-evolutionary relationships of
45 subviral agents with helper viruses.

46

47 **Keywords:** Co-evolution, dabbling duck, Hepatitis D virus, phylogeny

48

49

50 **Introduction**

51 Hepatitis delta virus (HDV) is a human-specific pathogen and the sole member of the
52 genus *Deltavirus*. The HDV genome is unique among known animal viruses but shares
53 similarities with plant subviral pathogens named viroids (1, 2). The single stranded, circular
54 RNA genome of HDV is approximately 1700 nucleotides and is therefore the smallest virus
55 infecting mammals. It is ~70% self-complementary, and forms a highly base paired rod-like
56 structure. It encodes two proteins (small and large delta antigen, S-HDAg and L-HDAg,
57 respectively) from a single open reading frame. HDV is regarded as a subviral pathogen that
58 requires the envelope proteins from the helper hepatitis B virus (HBV) for assembly and
59 release, and subsequently for entry into the host cell (2).

60 In humans, coinfection with HDV and HBV causes more severe liver disease than is
61 seen in individuals infected with HBV alone, and 15-20 million individuals are estimated to
62 be co-infected with both viruses (3, 4). There are currently 8 broad clades, or genotypes, of
63 HDV, with the greatest diversity found in Africa (5). However, the evolution of this virus is
64 poorly described, and its origin largely unknown (6). Current hypotheses for the origin of
65 HDV rely on host restriction, that is, that this virus is only found in humans and include:
66 viroid-like RNA having captured host signalling mRNAs (7), direct origination from the
67 human transcriptome (8), or evolution from a circular host RNA found in (1, 9). Given the
68 dependence of HDV on HBV for replication, there has likely been co-evolution between
69 HDV and the helper HBV, although the nature of this relationship has been largely
70 unexplored.

71 In this study we describe a divergent HDV-like agent found in wild birds and in the
72 absence of duck HBV. We demonstrate a number of features shared between HDV and this
73 avian HDV-like agent. This finding has important ramifications for our understanding of both
74 the origin and the co-evolutionary relationships of subviral agents and helper viruses.

75

76 **Results and Discussion**

77 As part of an avian meta-transcriptomic study we identified a genome related to that
78 of HDV, indicating that a novel and divergent HDV-like agent is present in the bird
79 population. RNA sequencing of the rRNA depleted library resulted in 20,945,917 paired
80 reads, which were assembled into 163,473 contigs, 279 of which were most similar to virus
81 sequences in the GenBank non-redundant protein database (nr). Avian viral transcripts were
82 highly abundant in the library, largely representing influenza A virus. RNA from an avian
83 HDV-like agent was ten-fold less abundant than that of influenza A virus, but was more

84 abundant than RNA from the host reference gene RPS13 that is stably expressed in ducks
85 (10) (Fig 1B). Exogenous duck hepatitis B virus (DHBV) was not identified in this meta-
86 transcriptomic library. The full genome of the novel avian HDV-like agent was represented
87 by a single contig (GenBank accession MH824555), wherein the virus genome was
88 duplicated, the result of sequencing a circular genome of 1706 nucleotides (Fig 1A). Unlike
89 HDV with a GC content of around 60% (11), the GC content of the avian HDV-like agent is
90 only 51%, with no significant peaks or troughs of GC content anywhere in the genome (Fig
91 1A). A conserved domain search identified the ORF in the virus genome as representing the
92 HDAg (e-value 3.40×10^{-10}). The predicted avian HDV-like protein (avHDAg) shares 32.2%
93 amino acid similarity to characterized HDAg proteins in the Genbank nr database. This
94 phylogenetic analysis indicated that avHDAg was highly divergent from all HDAGs encoded
95 by known human HDV genotypes (Fig 1C).

96 Despite this divergence, the avian HDV-like agent and HDV shared many features. In
97 accordance with the unbranched, rod-like genome structure described for HDV, we
98 demonstrate that the predicted that the circular RNA genome of the HDV-like agent also
99 folded into a classic unbranched rod-like structure (Fig. 2). Importantly, consistent with
100 HDV, the genome of the avian HDV-like agent had the capacity to express a protein,
101 avHDAg, and contained sequences reminiscent of the HDV genomic and antigenomic
102 ribozymes (12) and HDV-like ribozymes (13). To be consistent with the HDV nomenclature,
103 we regard the sequence with the avHDAg ORF as the antigenome. Given that the
104 antigenomic HDV ribozyme is located approximately 100 nucleotides downstream of the
105 small HDAg ORF in the 3'-direction, we examined the corresponding antigenomic region of
106 the avian HDV-like agent for the presence of ribozyme like sequences (avHDAg ORF
107 between nucleotides 1033 and 1590, Fig 1A). Two segments in the avian HDV-like genome
108 were identified as potential genomic and antigenomic ribozyme sequences. Their sizes and
109 locations are very similar to the ribozymes in the reference HDV genome sequence
110 (GenBank accession X04451.1) (Fig 1D, Fig 3). The potential genomic and antigenomic
111 ribozyme sequences were approximately 88 and 95 nt in length, respectively (compared to 85
112 and 89 nt of the human HDV ribozyme sequences (12)), and the calculated free energies were
113 -40.53 kcal/mol and -38.68 kcal/mol, respectively. When the inferred structures were re-
114 drawn based on the canonical secondary structures of the human HDV ribozymes (13), both
115 potential genomic and antigenomic duck ribozyme sequences displayed the ability to be
116 folded into classic HDV ribozyme secondary structures (Fig 3). This includes the five paired
117 (P) segments forming two coaxial stacks (P1 stacks on P1.1 and P4, while P2 stacks on P3),

118 with these two stacks linked by single-stranded joining (J) strands J1/2 and J4/2, as described
119 by (13).

120 The avian HDV-like genome contains a predicted ORF for the avHDAg which
121 encodes 185 amino acids. The start AUG is located within a Kozak consensus sequence with
122 a G in the +4 position, and Adenine in position -3 (14). Downstream of the coding sequence
123 after 105 nucleotides, the RNA genome encodes signals which are typical for the 3'-end of
124 eukaryotic mRNAs required for adding the poly(A) tail, the highly conserved 5'-AAUAAA
125 recognition sequence followed by the 5'-CA-3' cleavage sequence after 14 nucleotides (15,
126 16). In contrast to HDV, the genome of the avian HDV-like agent does not contain an editing
127 site as identified for HDV. For HDV, the editing event converts the 'UAG' stop codon into
128 the tryptophan 'UGG' codon (17), which extends the reading frame by an additional 18
129 amino acids, resulting in the synthesis of the L-HDAg. However, the avian HDV-like genome
130 potentially provides additional reading frames by +1 and +2 frame shifts extending the ORF
131 of 185 amino acids by 18 and 65 amino acids, respectively. The nucleotide sequence
132 encoding the additional 65 amino acids overlaps with the poly (A) signal sequence, and is
133 therefore less likely to be translated from a functional mRNA molecule. The C-terminal
134 region of the 185 amino acid protein, including the potential frame-shifted extensions do not
135 contain a C-X-X-X isoprenylation site, which is required for the synthesis of a functional L-
136 HDAg to support HDV assembly and release (18). Consistent with the presence of a coiled-
137 coil domain in the N-terminal region of the HDAg, the protein avHDAg also contains a
138 coiled-coil domain predicted in the N-terminal region between amino acids 22 and 44,
139 probably facilitating dimerization (Fig 4) (19, 20).

140 There are a number of hypotheses for the origin of HDV, including viroid-like RNA
141 captured host signalling mRNAs (7), that HDV originated directly from the human
142 transcriptome (8), or evolved from a circular host RNA found in hepatocytes that was able to
143 replicate (1, 9). A central component of these hypotheses is that HDV exists only in humans.
144 However, the discovery of an HDV-like genome in birds, with distinct similarities to the
145 HDV genome, such as self-complementarity and ribozyme folding, but also clear differences
146 (no ORF extension in the same frame downstream of the stop codon) suggests a divergent
147 evolutionary pathway of HDV and HDV-like pathogens. As we were not able to detect
148 DHBV genomes in the avian metatranscriptomic library, the identification of the genome of
149 the avian HDV-like agent in oropharyngeal and cloacal samples may indicate that the avian
150 HDV-like agent does not depend on a hepadnavirus for the completion of its replication
151 cycle. As such, the discovery of the genome of an avian HDV-like agent has important

152 implications for our understanding of both the origin and the co-evolutionary relationships of
153 the subviral agents with helper viruses, including the dependence of HDV on the HBV
154 envelope protein.

155

156 **Materials and Methods**

157 *Ethics statement*

158 This research was conducted under approval of Deakin University Animal Ethics Committee
159 (permit numbers A113-2010 and B37-2013). Banding was performed under Australian Bird
160 Banding Scheme permit (banding authority numbers 2915 and 2703). Research permits were
161 approved by Department of Environment, Land, Water and Planning Victoria (permit
162 numbers 10006663 and 10005726).

163

164 *Sample selection, RNA library construction and sequencing*

165 Waterfowl were captured at the Melbourne Water Western Treatment Plant, Victoria,
166 Australia, in 2012-13. Oropharangeal and cloacal samples were collected from Grey Teal
167 (*Anas gracilis*), Chestnut Teal (*A. castanea*) and Pacific Black Ducks (*A. superciliosa*) with
168 no signs of disease. RNA was extracted using the MagMax *mir*Vana Total RNA isolation Kit
169 (Thermo Scientific), assessed for RNA quality, and 10 samples with the highest concentration
170 were pooled using equal concentrations using the RNeasy MinElute Cleanup Kit (Qiagen).
171 Libraries were constructed and sequenced as per Shi *et al.* 2016 (21). Reads have been
172 deposited in the Short Read Archive BioProject PRJNA472212.

173

174 *RNA virus discovery*

175 Contigs were assembled, identified, and abundance calculated as per Shi *et al.* 2016 (21).
176 Briefly, sequence reads were demultiplexed and trimmed with Trimmomatic followed by *de*
177 *novo* assembly using Trinity (22). No filtering of host/bacterial reads was performed before
178 assembly. All assembled contigs were compared to the entire non-redundant nucleotide (nt)
179 and protein (nr) database with using blastn and Diamond (23), respectively, setting an e-value
180 threshold of 1×10^{-10} to remove potential false positives. Abundance estimates for all contigs
181 were determined using the RSEM algorithm implemented in Trinity. All contigs that returned
182 blast hits with paired abundance estimates were filtered to remove all bacterial and host
183 sequences. The virus list was further filtered to remove viruses with invertebrate (21), plant
184 or bacterial host association using the Virus-Host database
185 (<http://www.genome.jp/virushostdb/>).

186 To compare viral abundance to that of the host, a blast database was created containing
187 Ribosomal Protein S13 (RPS13) from both Mallard (taxid: 8839) and Chicken (*Gallus*
188 *gallus*) (taxid: 9031), which has found to be stably expressed in the Mallard (*Anas*
189 *playrhynchos*) lower gastrointestinal tract (10).

190

191 *Characterization of novel Hepatitis D-like virus*

192 Contigs greater than 1000bp in length were inspected (Geneious R10). Virus reads were
193 mapped back to the HDV-like contig using the Geneious mapping function to corroborate the
194 contig sequence and to calculate read coverage. Open reading frames were predicted within
195 Geneious, and interrogated using the conserved domain database (CDD,
196 <https://www.ncbi.nlm.nih.gov/Structure/cdd/wrpsb.cgi>), with an expected value threshold of
197 1×10^{-5} . Reference sequences of Hepatitis D representing all eight major clades were
198 downloaded from GenBank (Table S1). The translation of the HDAg proteins were aligned
199 using MAFFT (24), and gaps trimmed using trimAL (removing gaps that occur in more than
200 20% of sequences or with a similarity scores lower than 0.005, unless this removes more than
201 40% of columns) (25). Maximum likelihood trees were estimating using PhyML 3.0 (26),
202 incorporating the best-fit amino acid substitution model, here JTT +G+F, with 1000 bootstrap
203 replicates using the Montpellier Bioinformatics Platform ([http://www.atgc-](http://www.atgc-montpellier.fr/phym/)
204 [montpellier.fr/phym/](http://www.atgc-montpellier.fr/phym/)).

205 The avian HDV-like agent was subsequently interrogated for conserved features of
206 human HDV. At the genomic level, GC content want calculated within Geneious using a
207 sliding window of 10. To ascertain whether the circular genome folded into a classical
208 unbranched rod structure we utilized a RNA folding algorithm implemented on the mfold
209 webserver (27). The identification of the avian HDV-like agent ribozyme was performed in
210 two phases. The TT2NE algorithm was first applied on the genomic and antigenomic
211 ribozyme sequences of the reference HDV genome (GenBank accession X04451.1), and
212 although the models inferred by TT2NE were inaccurate (13), their topologies were distinct
213 and were used as references for screening. The free energy calculated for the HDV genomic
214 and antigenomic ribozyme sequences were -47.35 kcal/mol and -36.70 kcal/mol, respectively.
215 We screened incremental windows of 100 nt starting from first position of the antigenome of
216 the avian HDV-like agent, also including the complementary genomic sequences, with the
217 TT2NE algorithm to locate the potential ribozyme sequences. The incremental size was 50 nt
218 from positions 1 to 500 of the genome sequence and then 10 nt from position 500. All
219 inferred secondary structures that had free energy values similar to the reference models were

220 further evaluated using PseudoViewer (28). Coiled-coil structures of the ORF were identified
221 using Multicoil (29).

222

223 Acknowledgements

224 We are grateful to members of the Centre for Integrative Ecology at Deakin University for
225 sample collection and Melbourne Water for logistic support. This work was supported by an
226 ARC Discovery Grant (DP160102146). ECH is supported by an ARC Australian Laureate
227 Fellowship (FL170100022) and the Melbourne WHO Collaborating Centre for Reference and
228 Research on Influenza is funded by the Australian Department of Health.

229

230 References

- 231 1. **Taylor J, Pelchat M.** 2010. Origin of hepatitis delta virus. Future Microbiol **5**:393-
232 402.
- 233 2. **Taylor JM, Purcell RH, Farci P.** 2013. Hepatitis D (d) virus, p 2222-2241. In Knipe
234 DM, Howley PM (ed), Fields virology Lippincott Williams & Wilkins, Philadelphia,
235 USA.
- 236 3. **Wedemeyer H, Manns MP.** 2010. Epidemiology, pathogenesis and management of
237 hepatitis D: update and challenges ahead. Nat Rev Gastroenterol Hepatol **7**:31-40.
- 238 4. **WHO.** 2017. Hepatitis D fact sheet. World Health Organisation: media
239 centre:<http://www.who.int/mediacentre/factsheets/hepatitis-d/en/>.
- 240 5. **Le Gal F, Gault E, Ripault MP, Serpaggi J, Trinchet JC, Gordien E, Deny P.**
241 2006. Eighth major clade for hepatitis delta virus. Emerg Infect Dis **12**:1447-1450.
- 242 6. **Littlejohn M, Locarnini S, Yuen L.** 2016. Origins and Evolution of Hepatitis B
243 Virus and Hepatitis D Virus. Cold Spring Harb Perspect Med **6**:a021360.
- 244 7. **Brazas R, Ganem D.** 1996. A cellular homolog of hepatitis delta antigen:
245 implications for viral replication and evolution. Science **274**:90-94.
- 246 8. **Salehi-Ashtiani K, Luptak A, Litovchick A, Szostak JW.** 2006. A genomewide
247 search for ribozymes reveals an HDV-like sequence in the human CPEB3 gene.
248 Science **313**:1788-1792.
- 249 9. **Taylor JM.** 2014. Host RNA circles and the origin of hepatitis delta virus. World J
250 Gastroenterol **20**:2971-2978.
- 251 10. **Chapman JR, Helin AS, Wille M, Atterby C, Jarhult JD, Fridlund JS,**
252 **Waldenstrom J.** 2016. A panel of stably expressed reference genes for real-time
253 qPCR gene expression studies of Mallards (*Anas platyrhynchos*). PLoS ONE
254 **11**:e0149454. doi: 0149410.0141371/journal.pone.0149454.
- 255 11. **Wang KS, Choo QL, Weiner AJ, Ou JH, Najarian RC, Thayer RM, Mullenbach**
256 **GT, Denniston KJ, Gerin JL, Houghton M.** 1986. Structure, sequence and
257 expression of the Hepatitis Delta (Delta) viral genome. Nature **323**:508-514.
- 258 12. **Perrotta AT, Been MD.** 1991. A pseudoknot-like structure required for efficient self-
259 cleavage of Hepatitis Delta-Virus RNA. Nature **350**:434-436.
- 260 13. **Webb CHT, Luptak A.** 2011. HDV-like self-cleaving ribozymes. Rna Biology
261 **8**:719-727.
- 262 14. **Kozak M.** 1994. Determinants of translational fidelity and efficiency in vertebrate
263 mRNAs. Biochimie **76**:815-821.

264 15. **Proudfoot NJ.** 2011. Ending the message: poly(A) signals then and now. *Genes Dev* **25**:1770-1782.

265 16. **Hsieh SY, Taylor J.** 1991. Regulation of polyadenylation of hepatitis delta virus

266 antigenomic RNA. *J Virol* **65**:6438-6446.

267 17. **Casey JL, Bergmann KF, Brown TL, Gerin JL.** 1992. Structural requirements for

268 RNA editing in hepatitis delta virus: evidence for a uridine-to-cytidine editing

269 mechanism. *Proc Natl Acad Sci U S A* **89**:7149-7153.

270 18. **Glenn JS, Watson JA, Havel CM, White JM.** 1992. Identification of a prenylation

271 site in delta-virus large antigen. *Science* **256**:1331-1333.

272 19. **Xia YP, Lai MM.** 1992. Oligomerization of hepatitis delta antigen is required for

273 both the trans-activating and trans-dominant inhibitory activities of the delta antigen. *J*

274 *Virol* **66**:6641-6648.

275 20. **Lazinski DW, Taylor JM.** 1993. Relating structure to function in the hepatitis delta

276 virus antigen. *J Virol* **67**:2672-2680.

277 21. **Shi M, Lin XD, Tian JH, Chen LJ, Chen X, Li CX, Qin XC, Li J, Cao JP, Eden**

278 **JS, Buchmann J, Wang W, Xu JG, Holmes EC, Zhang YZ.** 2016. Redefining the

279 invertebrate RNA virosphere. *Nature* **540**:539-543.

280 22. **Grabherr MG, Haas BJ, Yassour M, Levin JZ, Thompson DA, Amit I, Adiconis**

281 **X, Fan L, Raychowdhury R, Zeng Q, Chen Z, Mauceli E, Hacohen N, Gnirke A,**

282 **Rhind N, di Palma F, Birren BW, Nusbaum C, Lindblad-Toh K, Friedman N,**

283 **Regev A.** 2011. Full-length transcriptome assembly from RNA-Seq data without a

284 reference genome. *Nature Biotech* **29**:644-652.

285 23. **Buchfink B, Xie C, Huson DH.** 2015. Fast and sensitive protein alignment using

286 DIAMOND. *Nat Methods* **12**:59-60.

287 24. **Katoh K, Standley DM.** 2013. MAFFT multiple sequence alignment software

288 version 7: improvements in performance and usability. *Mol Biol Evol* **30**:772-780.

289 25. **Capella-Gutierrez S, Silla-Martinez JM, Gabaldon T.** 2009. trimAl: a tool for

290 automated alignment trimming in large-scale phylogenetic analyses. *Bioinformatics*

291 **25**:1972-1973.

292 26. **Guindon S, Dufayard JF, Lefort V, Anisimova M, Hordijk W, Gascuel O.** 2010.

293 New algorithms and methods to estimate maximum-likelihood phylogenies: assessing

294 the performance of PhyML 3.0. *Syst Biol* **59**:307-321.

295 27. **Zuker M.** 2003. Mfold web server for nucleic acid folding and hybridization

296 prediction. *Nucleic Acids Research* **31**:3406-3415.

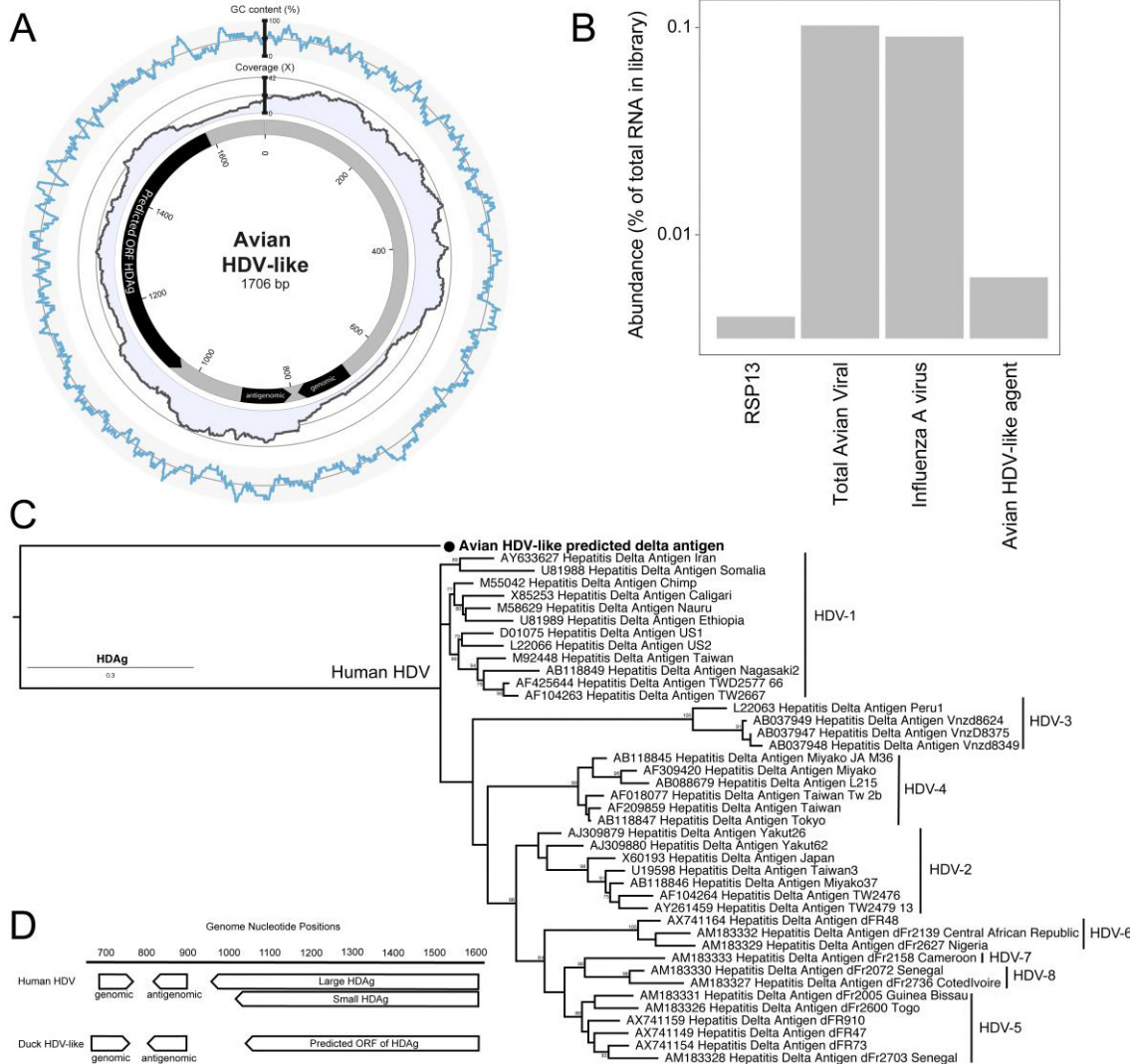
297 28. **Byun Y, Han K.** 2009. PseudoViewer3: generating planar drawings of large-scale

298 RNA structures with pseudoknots. *Bioinformatics* **25**:1435-1437.

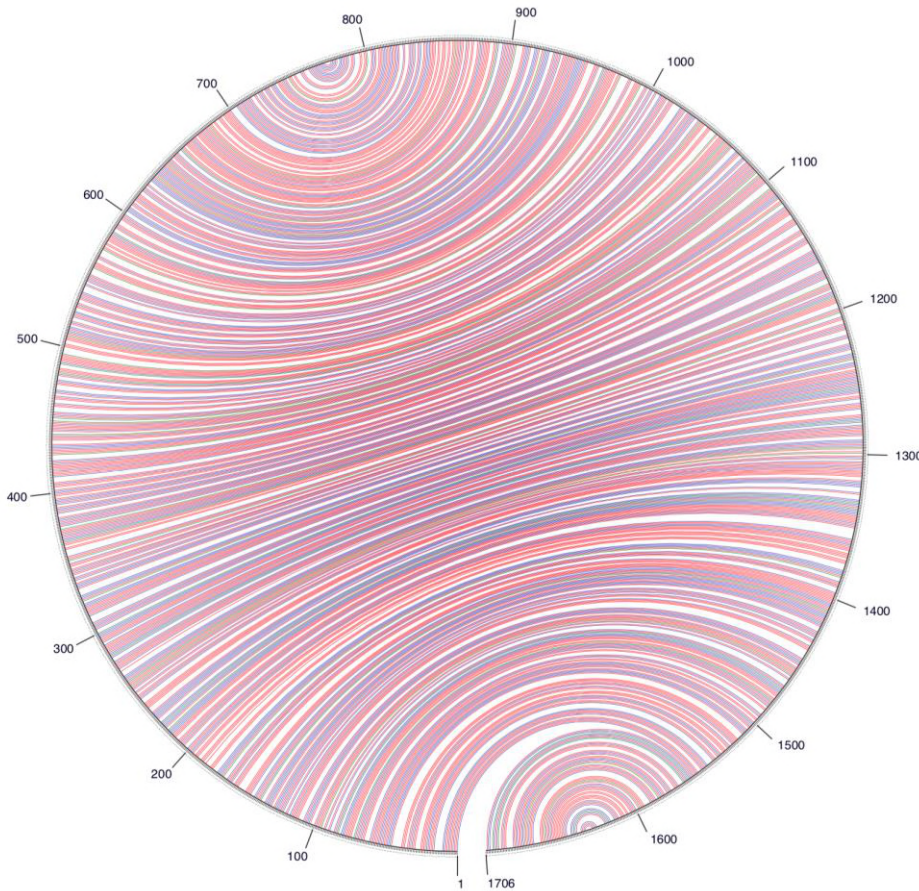
299 29. **Wolf E, Kim PS, Berger B.** 1997. MultiCoil: a program for predicting two- and

300 three-stranded coiled coils. *Protein Sci* **6**:1179-1189.

301



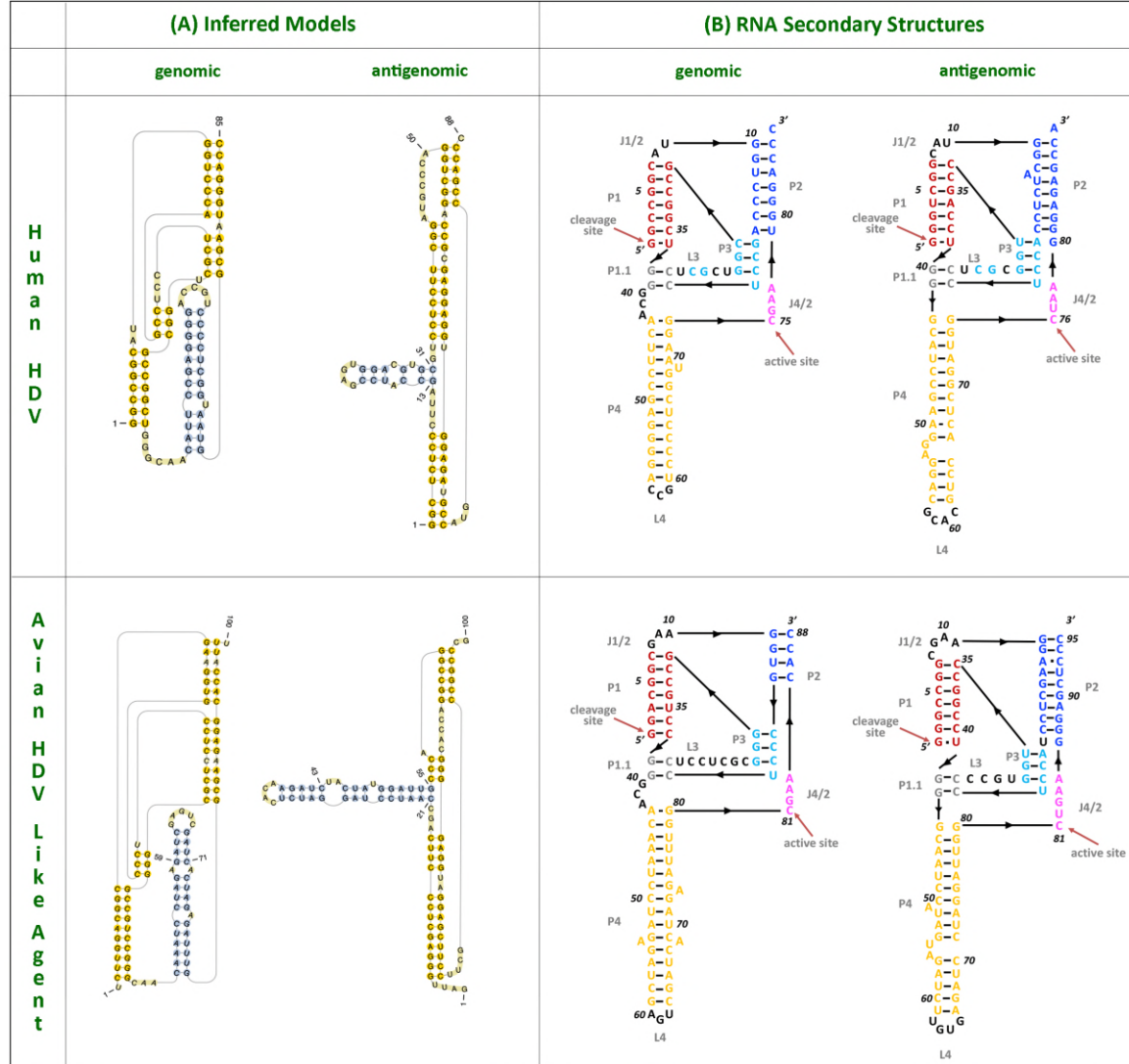
303
304
305 **Figure 1.** Characteristics of the genome of an avian HDV-like agent. (A) Avian HDV-like
306 agent genome, annotated with ORFs and genomic and antigenomic ribozyme sites. Metadata
307 rings include the read coverage, followed by GC content. (B) Abundance of transcripts in the
308 metatranscriptomic library. Total avian viral abundance was dominated by that of influenza A
309 virus. However, the abundance of HDV is higher than that of Ribosomal protein S13
310 (RPS13), a stably expressed reference gene in Mallards (*Anas platyrhynchos*). (C) Maximum
311 likelihood phylogeny of the HDAg protein. Representative human HDAg sequences included
312 fall into the currently described clades HDV1 - 8 (5). The scale bar represents the number of
313 amino acid substitutions per site. The phylogeny is rooted between the human and avian
314 viruses. (D) Location of genomic and antigenomic ribozyme sequences, and the predicted
315 ORF of the delta antigen in the avian HDV-like genome, compared to their location in the
316 HDV genome sequence (GenBank accession X04451.1).



317

318 **Figure 2.** A circle graph showing the base pairing of the circular RNA genome structure of
319 the avian HDV-like agent into an unbranched rod-like structure. The circle circumference
320 represents the genome sequence, and the arcs represent the base pairing. Colouring of arcs
321 are: red for G-C pairing, blue for A-U pairing, green for G-U pairing, and yellow for other
322 type of pairings.

323

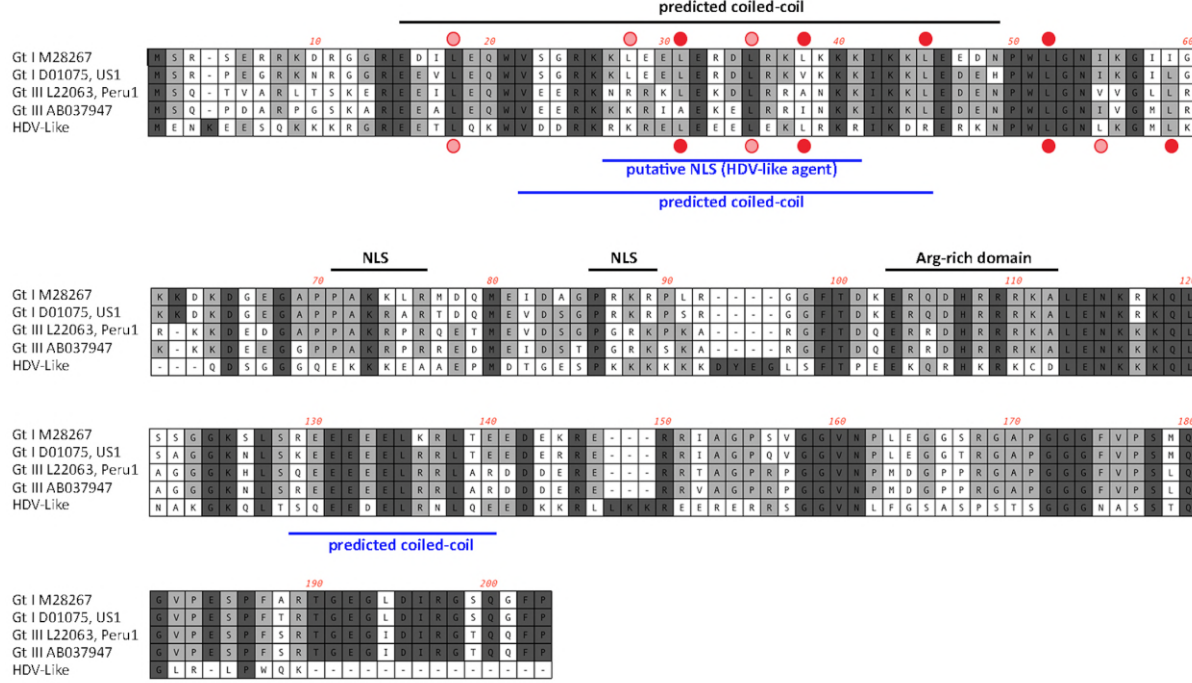


324

325 **Figure 3.** HDV ribozymes. (A) Secondary structures of the genomic and antigenomic
 326 ribozymes inferred using the TT2NE algorithm. The HDV ribozyme models were used as
 327 reference to screen for the ribozyme sequences in the avian HDV-like genome sequence. (B)
 328 Re-drawn secondary structures of the genomic and antigenomic ribozymes based on the
 329 secondary structures shown in review by Webb and Luptak (13).

330

331



332

333 **Figure 4.** Alignment of the amino acid sequences (small delta antigen) translated from the
 334 genomes of HDV and the avian HDV-like agent. The potential coiled coil region is
 335 highlighted, including the presence of leucines in a correct spacing for a leucine zipper (filled
 336 red circle). The delta antigen does not have a strict requirement for leucine in the d position
 337 of the heptad repeat. Additional leucines shown by circles in light red. NLS: Nuclear
 338 localisation signal.

339

340